

R. KUSTOSZ*, I. ALTYNTSEV*, M. DARLAK*, T. WIERZCHOŃ**, M. TARNOWSKI**, M. GAWLIKOWSKI*, M. GONSIOR*, M. KOŚCIELNIAK-ZIEMNIAK*

THE TIN COATINGS UTILISATION AS BLOOD CONTACT SURFACE MODIFICATION IN IMPLANTABLE ROTARY LEFT VENTRICLE ASSIST DEVICE RELIGAHEART ROT

WYKORZYSTANIE POWŁOK TIN JAKO ZMODYFIKOWANYCH POWIERZCHNI KONTAKTOWYCH W IMPLANTOWALNEJ ROTACYJNEJ KOMORZE WSPOMAGANIA SERCA RELIGAHEART ROT

Constructions of the mechanical-bearingless centrifugal blood pumps utilize different types of non-contact physical bearings, which allows to balance the forces that have an impact on the pump impeller, stabilizing its position in the pump house without wall contact. The paper presents investigations of the hybrid (passive magnetic bearings and hydrodynamic bearings) suspension system for the centrifugal blood pump. Numerical simulations were used to evaluate the hydrodynamic bearing lifting force and magnetic bearing forces interaction. An important aspect of rotor suspension system design was the nominal gap in hydrodynamic bearing area in order to reduce the blood damage risk in this region. The analyses results confirmed that for a small diameter centrifugal pump, the nominal operating hydrodynamic bearing gap could be established within the range from 0.033 to 0.072 mm.

Keywords: titanium nitride layers, athrombogenic coatings, implantable rotary pump, heart assistance

Konstrukcje pomp odśrodkowych pozbawionych łożysk mechanicznych wykorzystują różne rodzaje bezkontaktowych łożysk fizycznych, które pozwalają balansować siły oddziałujące na wirnik pompy, stabilizując jego pozycję w obudowie pompy bez kontaktu ze ścianami. Artykuł przedstawia badania hybrydowego (pasywne łożyska magnetyczne i łożyska hydrodynamiczne) systemu zawieszenia wirnika dla odśrodkowej pompy krwi. Symulacji numerycznych użyto dla zbadania siły unoszącej łożyska hydrodynamicznego oraz reakcji łożysk magnetycznych. Ważnym aspektem konstrukcji systemu zawieszenia wirnika było zwiększenie nominalnego prześwitu w obszarze łożyska hydrodynamicznego, aby zredukować ryzyko uszkodzenia krwi w tym rejonie. Wyniki analiz potwierdziły możliwość wyznaczenia nominalnego prześwitu w łożysku hydrodynamicznym, dla pomp odśrodkowych małej średnicy, w przedziale od 0,033 do 0,072 mm.

Introduction

Heart failure affects 23 million people worldwide, including 7 million patients in Europe, while the estimated Polish population is 1 million persons [1]. After over 50 years of clinical research, long term heart assist devices are widely clinically used for heart insufficiency treatment, as the bridge to heart transplantation, bridge to decision, bridge to recovery, either as destination therapy (DT) [2]. The heart transplant provides the gold standard in the end-stage of heart failure treatment. However, due to a persisting for over a decade lack of heart donor number growth, as well as increasing both a number of waiting patients and time for heart transplant – mechanical cardiac support (MCS) grows to be an important solution in heart failure treatment.

Over 12 thousands patients, with long term MCS devices have been registered in Interagency Registry for Mechanically Assisted Circulatory Support – INTERMACS, implanted since year 2006. The number of annual MCS implantations increased five times from the level of 500 cases in year 2007 to 2500 applications in year 2013, and is constantly dynamically rising, reporting annual implant number growth of 250 cases each year. The latest five year progress in this therapy has created a small revolution.

The implantable rotary blood pumps (IRBP) have become the absolute technology leader, with the first 459 implants INTERMACS registered in year 2008, followed with 2420 implants reported in year 2013 – containing 96,5% of all registered applications that year. The IRBP reliability, efficiency

* FOUNDATION OF CARDIAC SURGERY DEVELOPMENT, ARTIFICIAL HEART LABORATORY, ZABRZE, POLAND

** WARSAW UNIVERSITY OF TECHNOLOGY, SURFACE ENGINEERING DEPARTMENT, WARSAW, POLAND

and patient's life quality induce growth of MCS utilization as the DT heart failure treatment. The IRBP implantations covered 61% of total MCS applications registered in year 2009, with 59 implants applied as primary declared DT. The INTERMACS register of year 2013 reported 1052 DT primary applied MCS implantations, accompanied with the 100% MCS applications covered by IRBP, observed for the last 3 years [3].

The modern technology solution in IRBP belongs to miniaturized mechanical bearingless centrifugal pumps. The pump rotor is based on contactless suspension, utilizing different physical forces, while rotating with speed varied from 2000 to 6000

rotations per minute (rpm). Different types of the contactless bearings have been developed for the IRBP devices: active magnetic bearings [4], passive magnetic bearings, and hydrodynamic bearings [5]. The market leader of IRBP technology, the HVAD (Heart Ware Inc., USA) utilizes dynamic balancing of magnetic versus hydrodynamic forces, for rotor suspension in the middle of HVAD house with a gap of 0.075 to 0.5 mm [6] between the rotor and the house. The ReligaHeart ROT (RH ROT) rotary left ventricle assist device (LVAD) is the original IRBP device developed by Artificial Heart Laboratory of Zbigniew Religa Foundation for Cardiac Surgery Development, Zabrze, Poland.

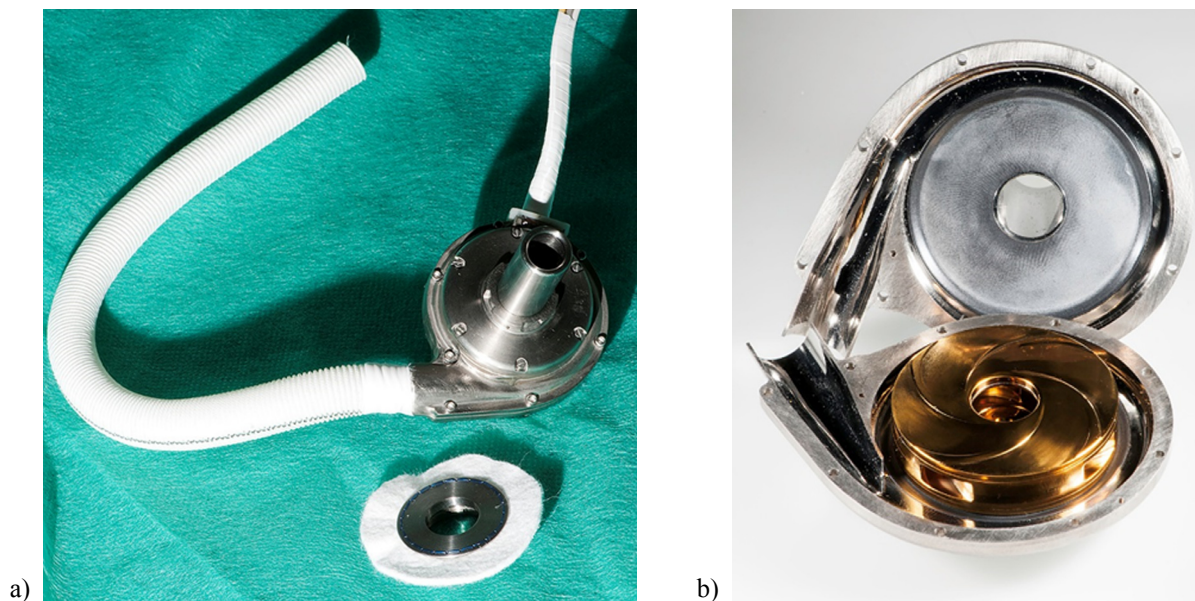


Fig. 1. The ReligaHeart ROT left ventricle implantable rotary pump: a) general view; b) internal view

The RH ROT consists of low profile impeller, suspended in the middle of the pump house, with a symmetric gap of 0,15 mm nominal distance on each side between the pump house and the impeller. The jointly acting static magnetic and hydrodynamic forces are used for impeller suspension, while rotating with the speed from 2000 to 5000 rpm.

The risk of blood cells damage as well as platelet activation, caused by cells exposure to high level of wall shear stress, makes the hydraulic rotor levitation system design exceptionally complex. Properly constructed non-contact physical bearing for IRBP device should provide the required level of impeller lifting force – to prevent a contact between the impeller and the pump house. The blood flow path, as well as, blood contacting elements of pump construction, should prevent blood cells damage and clotting activation, at the same time. The pump house and rotor material surface structure properties determine both the response of blood cells contacting rotor in high wall shear stress, as well as the result of incidental rotor-house contact. A few times higher blood flow velocity close to the pump rotor surface, compared to vessels wall physiologic flow condition, causes shear stress (SS) activating platelets and blood coagulation. The special micro-porous surface of pump elements is

necessary to reduce the SS against blood cells and embolization risk. The advanced surface engineering needs to be applied to modify the rotor and pump house material surface structure, to create efficient tribological conditions for blood and pump itself, stable during long term work.

Methods

The RH ROT device consists of low profile, 34 mm diameter and 8,2 mm high rotor, suspended in the middle of pump house, utilizing jointly acting static magnetic and hydrodynamic forces to create a symmetric gap between the pump house and the impeller, while rotating with speed from 2000 to 5000 rpm.

The RH ROT motor construction (Fig. 2) consists of two symmetrically located stators (see 6 at Fig. 2), joining 9 coils with the iron core (see 7 at Fig. 2), and 12 permanent magnets (see 7 at Fig. 2) located in rotor. The magnets are located within the impeller body, while the motor stator with coils is placed within the pump house. Doubling the electrical motor assembly in the pump construction allows to increase the pump reliability.

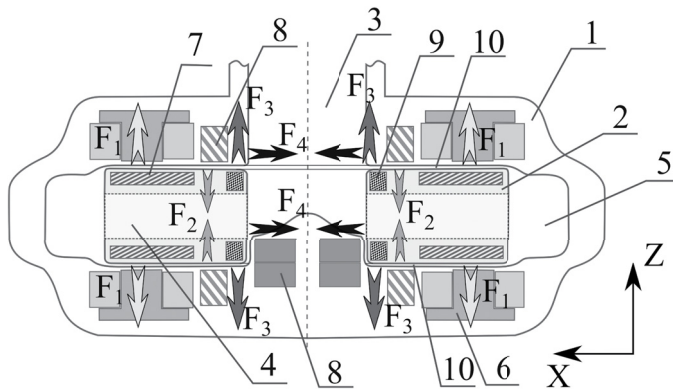


Fig. 2. The ReligaHeart ROT device diagram: 1 – pump house; 2 – pump rotor; 3 – blood inflow channel; 4 – impeller blood flow channel; 5 – spiral blood collecting outflow channel; 6 – motor stator; 7 – motor magnets; 8 – permanent magnetic bearings pump house magnets; 9 – permanent magnetic bearings rotor magnets; 10 – gap between pump house and impeller; F1 – motor magnets attracting force of motor stator; F2 – hydraulic bearings lifting force; F3 – permanent magnetic bearing axial force; F4 – permanent magnetic bearing radial force

Single motor is able to maintain the impeller rotation, providing redundancy in case of other motor malfunction.

The impeller suspension system was developed as the structure of permanent magnetic bearings, avoiding radial rotor displacement and sustaining it axial position in the middle of pump house, combined with hydraulic bearings, protecting impeller collision with the pump house.

The main role of the permanent magnetic bearings is to provide stable impeller position in radial direction. Construction of the magnetic bearings is based on the neodymium ring magnets, axially magnetized. Permanent magnetic bearings create the radial force F_4 (Fig. 2), forcing impeller rotation axis and pump house axis positions to be congruent. The permanent magnetic bearings control the impeller axial base position in the middle of pump house, utilizing axial force F_3 (Fig. 2). The motor attracting forces and any incidental impeller movement towards the pump house (precession, gravitation) is counteracted by hydraulic bearings lifting force F_2 (Fig. 2). Both numerical calculation and experimental measurements, at several stages of designing process were used for impeller suspension system development. Experimental measurements on the special test stands were used to validate the FEM numerical calculations and to confirm the force values in the system. The hydrodynamic bearings construction and characteristics were obtained by means of the CFD calculations, performed for different work parameters. The main goal of the constructing process of the hydrodynamic bearings was to provide the highest possible value of the bearing lift force (which balances the attractive forces between impeller, motor and bearing elements) to make sure that the gap between the impeller and pump casing is as wide as possible. To evaluate the hydrodynamic thrust force dependence on the pump work parameters (head of pump, rotational velocity) and bearing gap, the series of the calculations were performed. Hydrodynamic bearing lift force F_2 depends on the bearing geometry, fluid viscosity, clearance height, and rotational velocity. The calcu-

lations were performed for different rotational velocities, with the non-Newtonian fluid simulating blood – viscosity is related to the shear stress, with relation described by equation [1]. To obtain the force characteristics as a function of the bearing gap, calculations at different clearances (from 0.03 mm to 0.15 mm) were performed.



Fig. 3. The physical model for blood rotating with different rotational velocity over a biomaterial surface

The steady state numerical calculations were performed for the separated regions of the narrow gaps between the pump impeller and the pump house, to validate hydrodynamic conditions. The unstructured mesh, with the thin prismatic layer containing approximately 13 million elements, was used to calculate the flow in narrow gaps between the impeller and the pump house. The mesh independence tests, including the coarse and fine mesh, were performed confirming correctness of the selected mesh resolution. The SST turbulence model was used in the calculations.

The surface engineering was utilized to create structure and physicochemical status of blood pump elements surfaces, providing required biological properties and functions. The titanium nitride TiN+Ti₂N+Ti(N) layers were produced on titanium elements (roughness varied from micro- to nano-scale), by glow discharge process at plasma potential. The TiN surfaces were examined using SEM and AFM.

Thrombocytes exposed to SS were examined to evaluate biomaterials surface structure impact on the generated SS in rotary motion with different rotational velocities. The special physical model was developed as a chamber with rotating biomaterial disc (Ø 28 mm), simulating rotary pump rotor (Fig. 3). A distance of the disc to the chamber bottom was from 0,05 to 0,30 mm. Disc to chamber bottom distance was changed from 0,05 to 0,30 mm. Disc rotation speed was from 500 to 5000 rpm. Controlled blood flow was provided through the chamber; from 1 to 15 ml/min. The numerical analysis of flow conditions and shear stress was performed. The shear stress exposed thrombocytes activity was determined. Platelet activation was investigated using flow cytometry. The biomaterial surface after contact with blood was evaluated, using fluorescent and confocal microscopy.

Results

Bearing construction

The hydrodynamic bearing construction, consisting of 4 bearing blades was determined and developed (Fig. 4).

The numerical analysis showed hydrodynamic pressures created by bearing blades as the lifting force from 2 to almost 10 kPa, for nominal rotation speed = 3000 rpm (Fig. 5).

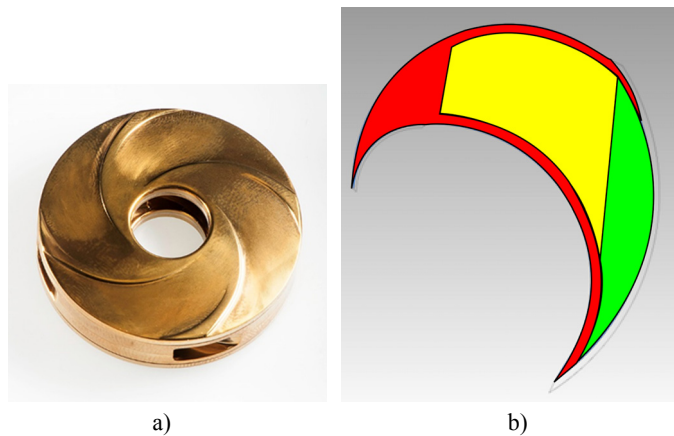


Fig. 4. Hydraulic bearings construction: a) hydraulic bearings picture; b) hydraulic bearing blade areas: green – bearing inlet; yellow – bearing lifting surface; red – bridging surface

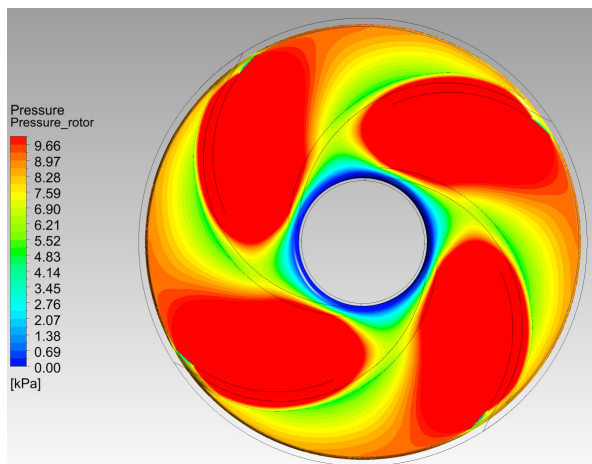


Fig. 5. Hydraulic bearing lifting pressures numerically determined for impeller rotation speed of 3000 rpm

The response characteristic of hydrodynamic bearing force against the cumulated magnetic force measured for different RGH ROT device operational conditions is presented in Figure 6.

The cumulated magnetic force represents the sum of the motor-impeller attracting force and permanent magnetic bearings forces. The hydrodynamic bearing lifting forces are presented for three different impeller rotation speeds: 2000, 3000, and 4000 rpm. The distance of the rotor to the pump house proper for balancing cumulated magnetic force by hydraulic forces is from 0,033 mm to 0,072 mm for rotation speed in the range from 2000 to 4000 rpm, respectively.

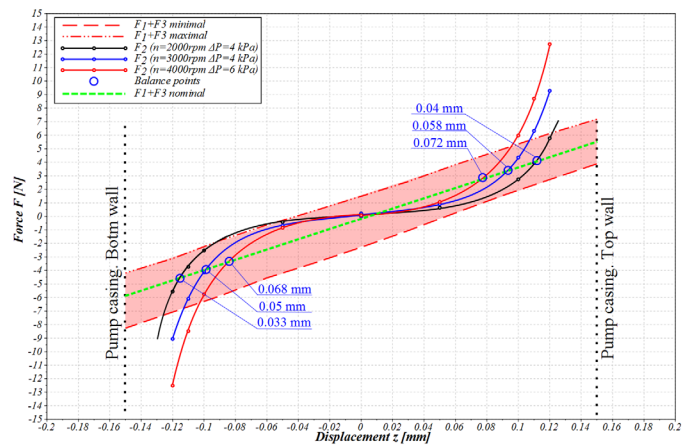


Fig. 6. The RH ROT impeller suspension forces reaction: F1 – motor magnets attracting force of motor stator; F2 – hydraulic bearings lifting force of different impeller rotation speed (red – 2000 rpm, blue – 3000 rpm, black – 4000 rpm); F3 – permanent magnetic bearing axial force

The numerically determined wall shear stress produced on the hydraulic bearing blade elements surface (bearing inlet, bearing lifting surface, bridging surface – Fig. 4) showed the shear stress values from 0,00 to 0,048 kPa (Fig. 7). The shear stress exceeding 0,2 kPa occurred only on a small area of bearing closure surface.

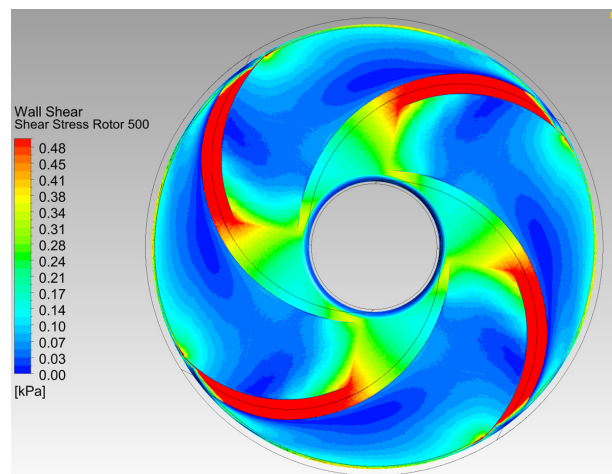


Fig. 7. Shear stress in hydraulic bearings area numerically determined for impeller rotation speed of 3000 rpm

TiN surface layers application

The developed glow discharge surface treatment, performed within 4 hour process at plasma potential in Nitrogen active atmosphere hydrogen supplementation, at the temperature of 830°C and pressure of 50 Pa, has allowed to produce diffusive TiN micro-layer on titanium, with controlled surface topography in micro and nano-scale. The TiN layer were manufactured on the different three dimensional rotary blood pump elements (Fig. 8: on the blood pump house (a), as well as on the rotor core (b), and hydraulic bearings surface (c)).

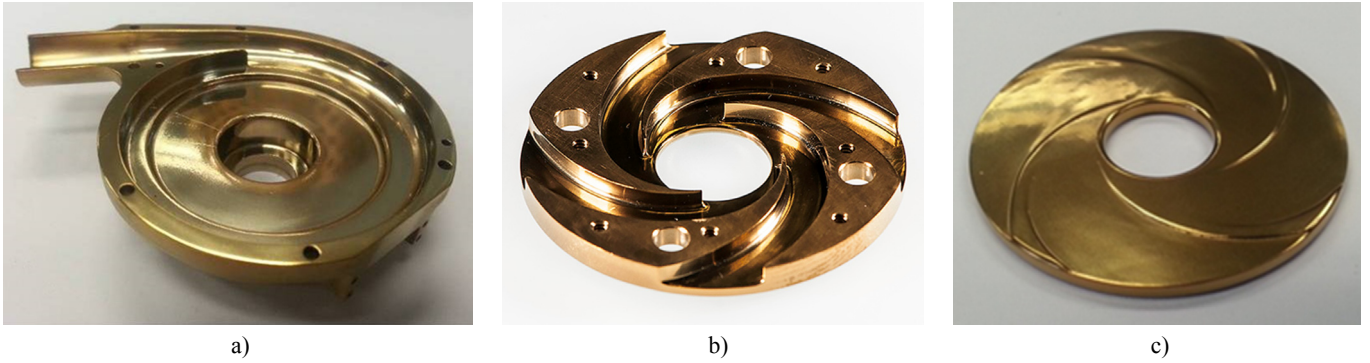


Fig. 8. ReligaHeart ROT device elements with TiN layer modified surface: a) pump house; b) half of impeller core with blood flow channel; c) impeller cover with blades of hydraulic bearing

The AFM analysis of all investigated hydraulic bearing areas, showed the surface roughness with attitude range variation of $\pm 0,5 \mu\text{m}$ around nominal value (Fig. 9 sections: b-e). The SEM analysis of investigated hydraulic bearing areas (points

from a to d) showed homogenous thickness of $13 \mu\text{m}$ thick TiN diffusive layer. (Fig. 9, sections f, g).

The roughness of blood pump TiN layers showed homogeneity on the whole modified surface, despite the complex blood

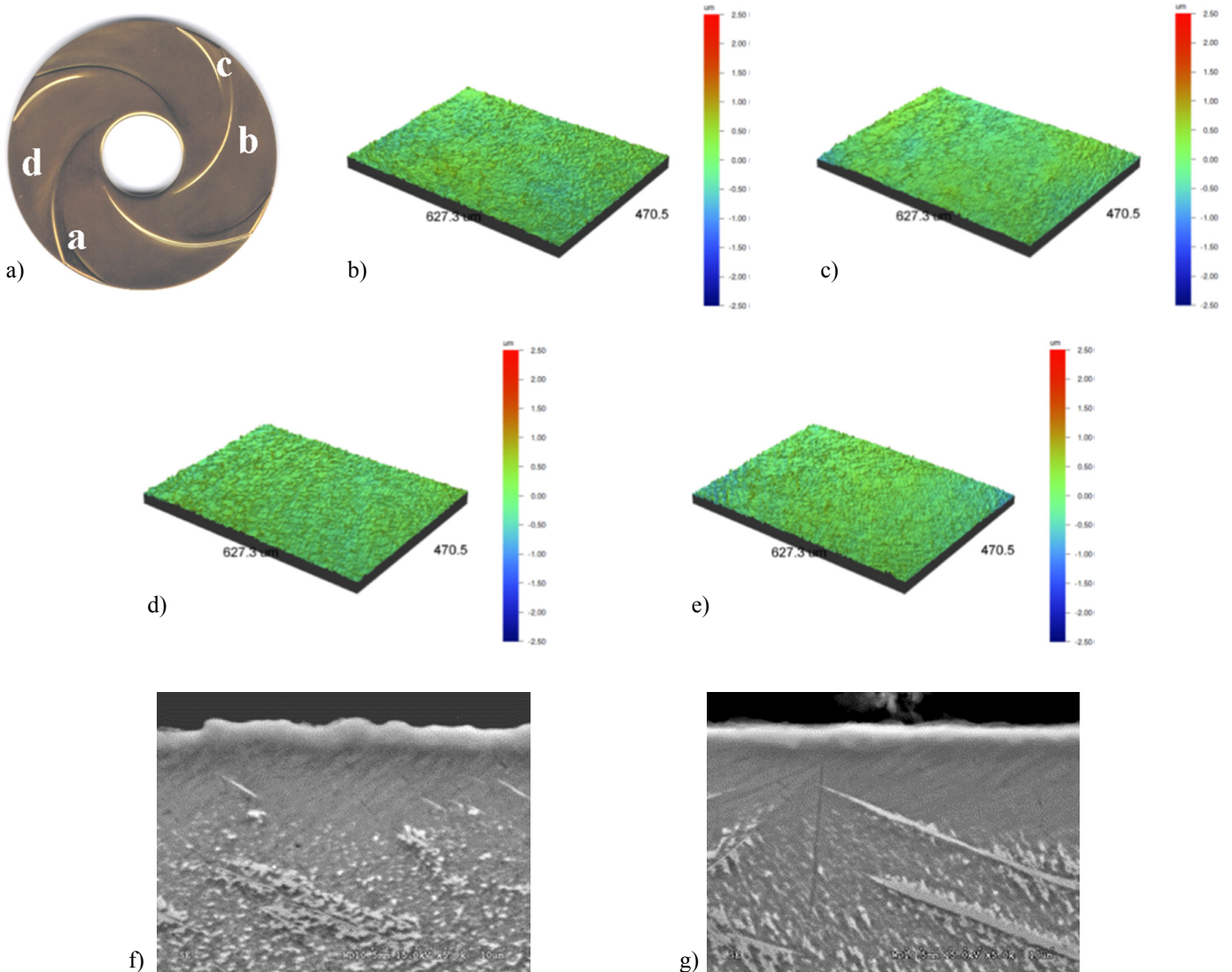


Fig. 9. The TiN layers structure on different areas of hydraulic bearing surface: a) the measuring areas determination – points marked a, b, c, d; b) AFM picture of surfaces roughness rotor area – a; c) AFM picture of surfaces roughness rotor area – b; d) AFM picture of surfaces roughness rotor area – c; e) AFM picture of surfaces roughness rotor area – d; f) SEM picture of layer cross section rotor area – a; g) SEM picture of layer cross section rotor area – d

pump elements' shape, for example, hydraulic bearing blades surface (Fig. 9), (Tab. 1). The hydraulic bearing surface had in all areas, namely, bearing inlet (Fig. 9a; Tab. 1-a), bearing lifting surfaces (Fig. 9b, d; Tab. 1-b, d), and closure surface (Fig. 9c; Tab. 1-c) similar roughness, represented with Ra value from 0,12 to 0,14 μm ; Rq value from 0,16 to 0,19 μm , Rz distance from 1,16 to 2,03 μm , with the maximum height of the profiles from 1,89 to 2,25 μm .

TABLE 1

Surface roughness parameters of TiN coated different areas of rotor hydraulic bearing: a, b, c, d – areas of hydraulic bearings (see Fig. 9a); Ra – arithmetic average of deviations absolute value; Rq – root mean squared of deviations absolute value; Rz – arithmetic average of distance between the highest peak and lowest valley in each sampling length; Rt – the maximum height of the profile

Measurement point	Ra [μm]	Rq [μm]	Rz [μm]	Rt [μm]
a	0,13	0,16	1,16	2,12
b	0,12	0,16	1,72	1,89
c	0,12	0,16	1,88	2,07
d	0,14	0,19	2,03	2,25

The plasma potential TiN modified surfaces, with reduced surface roughness (both Ra and $Rq < 200$ nm), presented the lower thrombocytes activation and adhesion to the biomaterial surface, in comparison with stainless steel. The haemolytic and trombogenicity examination results analysis demonstrated that diffusive TiN+Ti₂N+ α Ti(N) layer produced on titanium surface does not cause erythrocytes damage (Fig. 10) and platelets adhesion (Fig. 11) in the dynamic high shear stress conditions.

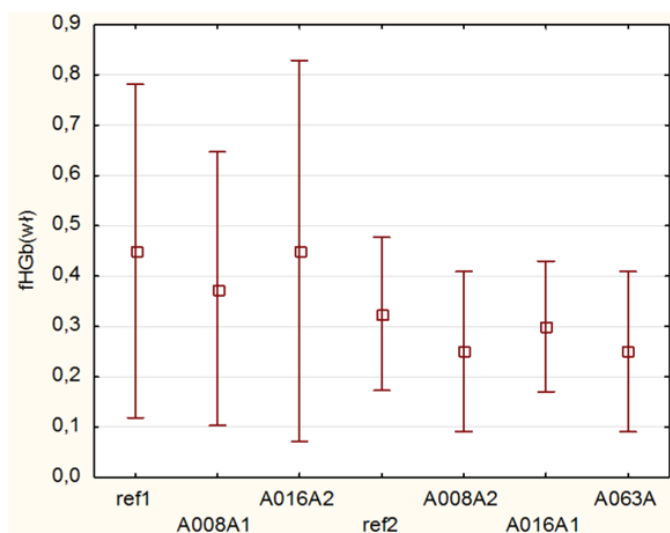


Fig. 10. The free haemoglobin level reported in blood after single exposure to high shear stress, produced experimentally by different TiN modified titanium Grade2 surfaces: ref1, ref2 – Titanium Grade 2 reference samples, roughness 0,08 μm ; A008A1 – TiN layer (created at cathode potential) with $Ra = 0,08$ μm ; A016A2 – TiN layer (created at cathode potential) with $Ra = 0,16$ μm ; A008A2 – TiN layer (created at plasma potential) with $Ra = 0,08$ μm ; A016A1 – TiN layer (created at plasma potential) with $Ra = 0,16$ μm ; A063A – TiN layer (created at plasma potential) with $Ra = 0,63$ μm

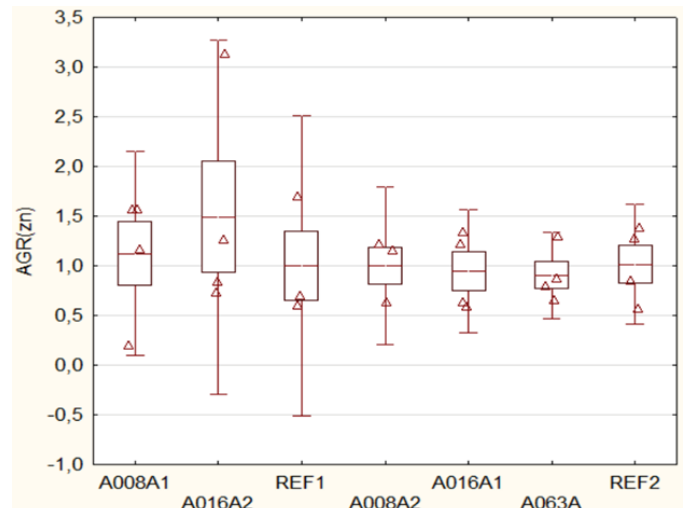


Fig. 11. The platelets aggregation level reported in blood after single exposure to high shear stress, produced experimentally by different TiN modified titanium Grade2 surfaces: ref1, ref2 – Titanium Grade 2 reference samples, roughness 0,08 μm ; A008A1 – TiN layer (created at cathode potential) with $Ra = 0,08$ μm ; A016A2 – TiN layer (created at cathode potential) with $Ra = 0,16$ μm ; A008A2 – TiN layer (created at plasma potential) with $Ra = 0,08$ μm ; A016A1 – TiN layer (created at plasma potential) with $Ra = 0,16$ μm ; A063A – TiN layer (created at plasma potential) with $Ra = 0,63$ μm

Discussion

Different bearing types have been used in the rotary blood pump constructions state of the art. The 2nd generation pumps (axial flow pumps mainly) have used mechanical sliding bearings [7]. The 3rd generation pumps (both axial and centrifugal pumps) are equipped with the non-contact physical bearings [8]. Each of the mentioned above bearing concepts has both advantages and disadvantages.

Mechanical contact bearings ensure the high precision of the impeller positioning in the pump house cavity and provide high reliability of the impeller position. They are widely used in the axial blood pumps, with reduced risk of blood clot formation in the low flow area a bearing, due to positioning of the bearing in the main blood flow path [9]. Utilization of mechanical bearings in the centrifugal blood pumps can lead to clot formation between the impeller and the pump case, as a consequence of flow speed reduction and the increased time of blood cells residence in the bearing area.

Symmetrical construction of the rotor and motor of ReligaHeart ROT device leads to symmetrical characteristic of the force attracting the motor core and permanent magnets. The static motor attracting force characteristic is constant - does not depend on the pump operation condition. It is determined by magnetic parameters of the motor core and permanent magnets. The unstable equilibrium position is located in the middle of the distance between the top and bottom wall of the pump house cavity.

As mentioned above, the sum of the motor attractive force F_1 and axial force of the permanent magnetic bearings F_3 defines the values of the axial imbalance force. The wide range of the

bearing axial force characteristics could be obtained, due to adjusting the position of the bottom magnetic bearings. Therefore, the acceptable range of the axial imbalance force was obtained (shaded area in Fig. 5).

The hydrodynamic bearings lifting force characteristics for three impeller rotational speeds, and corresponding minimal possible pressure differences are presented in Figure 5. The lowest values of the pressure head in the pump cavity, related with current rotational speed, were used in calculations – to simulate the worst bearing operational conditions. Increasing the pump head in parallel with the decreasing pump flow rate leads to increasing the hydrodynamic bearings lifting force. Apparently, the smallest values of the lifting force have been achieved for rotational speed of 2000 rpm, and pump head of 4 kPa. Such operational conditions correspond to the smallest possible values of the lifting force, observed during normal pump operating. The balance between the hydrodynamic bearing force as well as imbalance forces in this situation (presented in Fig. 5) could be achieved when the bearing clearance is 0.03 mm towards the top pump house wall, and 0.022 mm towards the bottom pump house wall. It should be mentioned that these points represent

the worst case of force level, in sense that the attracting forces between the impeller and pump house are maximal. Nominal operation setup of the bearing magnets will provide the nominal magnetic bearing axial force characteristic located in the shaded area (F3 in Fig. 5). In this case the values of the imbalance force will be reduced, and the hydrodynamic bearing gap will increase up to 0.04 mm and 0.033 mm, as a consequence, respectively. It will create a positive blood impact – reducing the shear stress level caused by hydrodynamic bearings against blood cells (reduction of shear stress maximal values) and reducing shear stress exposure time (reduce the blood cells residence time in the area of the bearings).

- The proposed system of the bearings was used in the prototype construction of the ReligaHeart ROT centrifugal pump (Fig. 1). The laboratory test confirmed both the pump performances and proper pump operation (including the bearings system). Experimental pump performance characteristics are presented in Figure 6. The prototype operational characteristics have showed that the pump reaches the maximal efficiency of 45%. Small mechanical losses in the pump confirm the proper operation of the bearings.

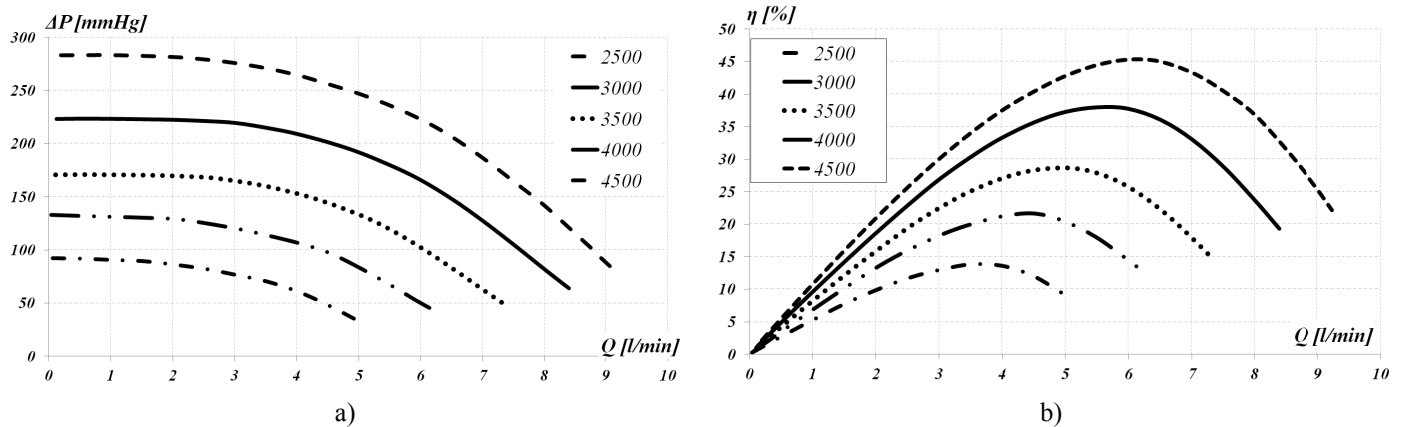


Fig. 12 Experimental RH ROT device characteristics a) head of the pump, b) pump efficiency

The titanium and titanium compounds are widely used as construction materials in implantable rotary blood pumps. They are assisted with advanced materials, like composites, for motor electro-magnetic efficiency increase, and with surface modification engineering to create blood cells compatible and long term durable blood contacting surfaces of pump elements. The technology leader HAVD pump (HeartWare, USA) utilizes the TiN coated layers just on impeller surface.

The TiN layers manufacturing process on titanium elements of ReligaHeart ROT device, utilizing glow discharge, showed that the TiN layer created in plasma potential process increased the original material roughness of the treated pump elements less than TiN layer created at cathode potential (Tab. 2). The R_a parameter increasing was 70% higher, comparing the effect

of cathode potential treatment to plasma potential treatment (R_a changed from 0,016 μm of the base value to 0,081 μm for TiN layer of cathode process and to 0,048 μm for TiN layer of plasma process, respectively). Additionally, the R_z parameter increasing was 60% higher, comparing the effect of cathode potential to plasma potential treatment (R_z changed from 0,021 μm of the base value to 0,099 μm for TiN layer of cathode process vs. to 0,062 μm for TiN layer of plasma process, respectively). Finally, the R_q parameter increasing was 39% higher – comparing TiN layer manufacturing at cathode potential to plasma potential (R_q changed from 0,253 μm of base value to 0,617 μm for TiN layer of cathode process, and to value 0,443 μm for TiN layer of plasma process, respectively).

TABLE 2

Surface roughness parameters of TiN coated; Ra – arithmetic average of deviations absolute value; Rq – root mean squared of deviations absolute value; Rz – arithmetic average of distance between the highest peak and lowest valley in each sampling length

Sample	Parameter	Ra [μm]	Rq [μm]	Rz [μm]	Investigated surface [μm^2]
Titanium Grade 2 polished		0,016	0,021	0,253	101,80
Titanium Grade 2 polished + TiN layer (cathode potential process)		0,081	0,099	0,617	106,23
Titanium Grade 2 polished + TiN layer (plasma potential process)		0,048	0,062	0,443	103,81

The biological investigation showed that positive results were established for every base Titanium surface roughness treated with TiN layer manufactured at plasma potential level. There were no significant differences in free haemoglobin level and platelet aggregation after shear stress exposure to TiN treated samples, with base material surface roughness Ra index varied from 0,08 μm through 0,016 μm to 0,063 μm (see Fig. 10 and 11). Those results suggested that the pump element manufacturing quality regarding surface polishing was not critical when blood contact surfaces were modified with TiN layer, plasma potential glow discharge created. The fundamental for blood contact surface properties was the TiN layer surface modification, performed as the plasma potential glow discharge treatment.

Conclusion

The presented results of the numerical calculations and experimental measurements of the force characteristics for different bearings allowed to construct the contactless suspension system, comprising the hydrodynamic and magnetic bearings, and creating required levels of the lifting force. At the same time it allows to increase the clearance in hydrodynamic bearings area, and to reduce the negative impact of hydrodynamic bearings on the blood cells, as a consequence.

The developed glow discharge process at plasma potential has allowed to produce diffusive TiN micro-layer on titanium, with controlled surface topography in micro and nano-scale level. The several microns thick diffusive TiN layers were produced on the different three dimensional rotary blood pump elements:

rotors and blood pump house. The roughness of TiN layers showed homogeneity on whole modified surface, despite of the complex shape of blood pump elements. The thrombogenicity and haemolytic analysis of examinations results demonstrated that diffusive TiN+Ti₂N+ α Ti(N) layer produced on titanium surface does not cause erythrocytes damage and platelets adhesion in the dynamic high shear stress conditions.

Results obtained in prototype investigations promise good properties of the newly developed layers for application in blood contacting elements of rotary blood pumps, where blood velocity and shear stresses level could increase the risk of thrombosis.

The validation of the obtained results will be performed in further laboratory and biological experimental investigations of the ReligaHeart ROT pump prototype, equipped with developed impeller suspension system, as well as rotor and pump house blood contact TiN surface layers modified and created by glow discharge at plasma potential.

Acknowledgements

The research was performed within the national “Polish Artificial Heart” program, and research project PBS1/A5/20/2012; both funded by the National Centre for Research and Development.

REFERENCES

- [1] V.L. Roger, et al. *Circulation*. **e2-294**, 131 (2015).
- [2] C. Garrick, et al. *Circulation*. **125**, 1304 (2012).
- [3] J. K. Kirklin, et al, Sixth INTERMACS annual report: A 10,000 patient database; *JHLT*. **6**, 133 (2014).
- [4] K. Borque, Implantable blood pump, U.S. Patent; US 2012/0046514, 2011.
- [5] J.C. Woodard, et al., Rotary pump with hydro-dynamically suspended impeller, U.S. Patent; US2003/6609883 B2, 2003.
- [6] J. A. La Rose, et al; Stabilizing drive for contactless rotary blood pump impeller; U.S. Patent; US 2008/0021394 A1, 2008.
- [7] L.P. Taylor, et al., Implantable electric axial-flow blood pump with blood-cooled bearing, U.S. Patent; 5951263, 1999.
- [8] D. LaRose, M. Tamez, Ashenuga, C. Reyes. *ASAIO Journal*. **56(4)**, 285 (2010).
- [9] A. Loforte, A. Montalto, et al. *Journal of Cardiovascular Medicine*. **10(10)**, 765 (2009).